Validity of the effective Hamiltonian in the two-photon atom-field interaction

A. H. Toor and M. S. Zubairy
Department of Electronics, Quaid-i-Azam University, Islamabad, Pakistan
(Received 20 May 1991; revised manuscript received 31 October 1991)

Two-photon processes are usually treated using effective-Hamiltonian approaches. In this paper the question of the validity of the effective Hamiltonian in the interaction of a single atom with a single-mode radiation field is considered, and conditions under which effective and microscopic Hamiltonians lead to identical results for the reduced density matrix for the field are derived. The conditions and limitations for the validity of the effective Hamiltonian are elucidated by considering the population inversion, photon distribution function, and squeezing in the two approaches.

PACS number(s): 42.50.Dv, 42.50.Ar

I. INTRODUCTION

Two-photon processes in atomic systems are important in quantum optics due to the high degree of correlation between the emitted photons. This correlation may lead to the generation of nonclassical states of the electromagnetic field, such as squeezed states [1,2] and the violation of other classical inequalities [3]. In case of a two-photon laser, a rapid growth of field inside the cavity is predicted [4]. Several authors have discussed the possibility of observing sub-Poissonian photon statistics in the multiphoton-absorption processes [5]. Recently a two-photon micromaser has been operated which offers a chance to study, under controlled conditions, the interaction of a single mode of the electromagnetic field with a single atom [6].

For many years, the effective Hamiltonian approach (EHA) has been used to describe the two-photon processes in quantum optics. It is shown by Zhu and Li [7] that there are differences between results, depending on the diagonal elements of the reduced density matrix of the field obtained using the EHA and the full microscopic Hamiltonian approach (FMHA). Alsing and Zubairy have shown the collapses and revivals in the two-photon absorption process by adiabatically eliminating the intermediate states [8]. By using the microscopic Hamiltonian approach, some important work has been carried out. Recently a theory of the two-photon correlated-emission laser in a coherent superposition of the three-level atomic states has been developed [9]. The phase-sensitive amplification in a two-photon three-level atomic system leading to noise-free amplification in one quadrature component has also been studied [10]. A quantum theory of a two-photon micromaser has also been developed [11].

Recently there has been interest in studying the question of the validity of the effective Hamiltonian approach. For instance, Boone and Swain [12] have shown that the approaches based on the EHA and FMHA lead to the same equations for the diagonal elements of the field density matrix in a nondegenerate two-photon laser under certain conditions. Under these conditions, however, the off-diagonal elements of the reduced density matrix for the field do not give the same results. Ashraf, Gea-Banacloche and Zubairy [13] have presented similar results for a two-photon micromaser. However, it has been claimed that the difference between the two approaches is caused by the neglecting of the dynamic Stark shift in the effective Hamiltonian. Consequently, a modified effective Hamiltonian that includes the dynamic Stark shift through the inclusion of Stark parameters for both the atomic levels was proposed by Puri and Bullough [15], Lugiato, Galatola, and Narducci [16], and others.

In this paper we have discussed the limitations of the effective and the modified effective Hamiltonians. The conditions have been determined under which the effective Hamiltonians can be employed to study the degenerate two-photon processes. In Sec. II, we derive the probability amplitude equations for both the effective and the full microscopic Hamiltonian. The comparison of these two sets of equations under the conditions that the three-level atom of the FMHA effectively reduce to a two-level atom leads to an additional overall phase factor in the FMHA. We have presented a comparative study of the two approaches for the population inversion and the photon distribution function. We have considered the large-detuning limit for both the initial thermal and the coherent fields. It is shown that, under certain conditions, on atomic detuning and mean number of photons, the two approaches lead to identical results for these quantities. The role of the off-diagonal elements of the reduced density matrix of the field can be seen in the case of squeezing. We have compared the results for the variances in the two quadratures for the EHA and the FMHA for the case of initial coherent field. It is shown that, due to the presence of an additional overall phase factor, different results for squeezing are obtained in general in the two approaches. This clearly shows that the effective Hamiltonian approach is inadequate for the description of squeezing in the two-photon atom-field interaction. This is caused by the neglecting of the dynamic Stark shift in the EHA. In Sec. III, a modified [15,16] effective Hamiltonian approach (MEHA) is considered, which includes Stark parameters. We derive the probability amplitude equations for the MEHA and then compare them with those obtained from the FMHA. The conditions have been determined under which this modified effective Hamiltonian can be used to study the quantities in which both diagonal and off-diagonal elements of the reduced density matrix are involved.

II. PROBABILITY AMPLITUDES IN THE TWO-PHOTON JAYNES-CUMMINGS MODEL

We generalize the Jaynes-Cummings model to two-photon processes in the degenerate case and obtain a time-dependent solution for the probability amplitudes in both the effective and the full microscopic Hamiltonian approaches. We then derive the conditions under which the two approaches lead to identical expressions for the probability amplitudes within a phase factor. This additional phase factor is the result of the neglect of the dynamic Stark shift in the effective Hamiltonian. Then a modified effective Hamiltonian is considered in which the dynamic Stark shift is being taken care of. The necessary conditions are determined under which even this modified effective Hamiltonian could only be used to study the two-photon degenerate processes.

A. Effective Hamiltonian approach

We consider a single two-level atom interacting with a single-mode radiation field. The atomic levels $|a\rangle$ and $|c\rangle$ are coupled through the two-photon coupling constant λ, at exact resonance. The Hamiltonian in the interaction picture, under the rotating-wave approximation (RWA), is

$$H=\hbar\lambda(a^2|a\rangle\langle c|+a^{\dagger 2}|c\rangle\langle a|)\ , \tag{1}$$

where a and $a^\dagger$ are the field annihilation and creation operators, respectively.

The wave function for the combined atom-field system is

$$|\psi(t)\rangle=\sum_n [c_{a,n}(t)|a,n\rangle+c_{c,n}(t)|c,n\rangle]\ , \tag{2}$$

where states $|\alpha,n\rangle$ ($\alpha=a,c$) represent the atom in state $|\alpha\rangle$ and the field in Fock state $|n\rangle$, and $C_{\alpha,n}(t)$ are the corresponding probability amplitudes. It follows from the time-dependent Schrödinger equation, by using Eqs. (1) and (2), the probability amplitudes obey the following first-order coupled differential equations:

$$\dot{C}_{a,n}(t)=-i\lambda\sqrt{(n+1)(n+2)}C_{c,n+2}(t)\ , \tag{3}$$

$$\dot{C}_{c,n+2}(t)=-i\lambda\sqrt{(n+1)(n+2)}C_{a,n}(t)\ . \tag{4}$$

We assume that, at the initial time $t=0$, atom and field are decoupled, i.e.,

$$\begin{aligned} C_{a,n}(0)&=C_aC_n(0)\ ,\\ C_{c,n+2}(0)&=C_cC_{n+2}(0)\ , \end{aligned} \tag{5}$$

where $C_n(0)$ is the amplitude of the initial field, and

$$\begin{aligned} C_a&=\cos(\theta/2)\ ,\\ C_c&=\sin(\theta/2)\exp(-i\phi)\ . \end{aligned} \tag{6}$$

On varying θ and ϕ we can consider different situation; for example, $\theta=0$ means that the atom is initially in the excited state, while $\theta=\pi/2$ means that the atom is in the coherent superposition of states for a fixed value of ϕ, with ϕ being the relative phase between atomic states $|a\rangle$ and $|c\rangle$.

A solution of Eqs. (3) and (4), subject to the boundary condition (5), is given by

$$\begin{aligned} C_{a,n}(t)=&\cos[\sqrt{(n+1)(n+2)}\lambda t]C_{a,n}(0)\\ &-i\sin[\sqrt{(n+1)(n+2)}\lambda t]C_{c,n+2}(0)\ , \end{aligned} \tag{7}$$

$$\begin{aligned} C_{c,n+2}(t)=&\cos[\sqrt{(n+1)(n+2)}\lambda t]C_{c,n+2}(0)\\ &-i\sin[\sqrt{(n+1)(n+2)}\lambda t]C_{a,n}(0)\ . \end{aligned} \tag{8}$$

These are the expressions for the probability amplitudes using the EHA.

B. Full microscopic Hamiltonian approach

Next we consider a single three-level atom (see Fig. 1), in a cascade configuration, interesting with the single-mode radiation field. We assume exact two-photon resonance, such that the intermediate level $|b\rangle$ is detuned from the exact one-photon resonance. The detuning is given by

$$\Delta=\Omega-(\omega_a-\omega_b)=(\omega_b-\omega_c)-\Omega\ , \tag{9}$$

where Ω is the cavity resonant mode frequency and ω_a, ω_b, and ω_c are the frequencies associated with the atomic levels $|a\rangle$, $|b\rangle$, and $|c\rangle$, respectively.

The full microscopic Hamiltonian in the interaction picture is

$$\begin{aligned} H=&\hbar g_1[a|a\rangle\langle b|\exp(-i\Delta t)+a^\dagger|b\rangle\langle a|\exp(i\Delta t)]\\ &+\hbar g_2[a|b\rangle\langle c|\exp(i\Delta t)+a^\dagger|c\rangle\langle b|\exp(-i\Delta t)]\ , \end{aligned} \tag{10}$$

where g_1 and g_2 are the one-photon coupling constants for the transitions $|a\rangle-|b\rangle$ and $|b\rangle-|c\rangle$, respectively. The combined atom-field wave function is given by

$$\begin{aligned} |\psi(t)\rangle=\sum_n [&C_{a,n}(t)|a,n\rangle+C_{b,n}(t)|b,n\rangle\\ &+C_{c,n}(t)|c,n\rangle]\ . \end{aligned} \tag{11}$$

It follows from the time-dependent Schrödinger equa-

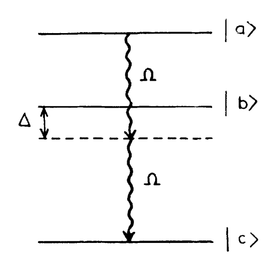

FIG. 1. Schematic diagram of the three-level atom interacting with the single-mode radiation field.

tion that the probability amplitudes obey the following first-order coupled differential equations:

$$\dot{C}_{a,n}(t)=-ig_1C_{b,n+1}(t)\sqrt{(n+1)}\exp(-i\Delta t)\ , \quad (12)$$

$$\dot{C}_{b,n+1}(t)=-ig_1C_{a,n}(t)\sqrt{(n+1)}\exp(i\Delta t) -ig_2C_{c,n+2}(t)\sqrt{(n+2)}\exp(i\Delta t)\ , \quad (13)$$

$$\dot{C}_{c,n+2}(t)=-ig_2C_{b,n+1}(t)\sqrt{(n+2)}\exp(-i\Delta t)\ . \quad (14)$$

We solve these differential equations by assuming, as earlier in the case of the EHA, that the atom and the field are decoupled at $t=0$ and the atom is present in a coherent superposition of states $|a\rangle$ and $|c\rangle$ only, i.e.,

$$C_{a,n}(0)=C_aC_n(0)\ ,$$
$$C_{b,n+1}(0)=0\ , \quad (15)$$
$$C_{c,n+2}(0)=C_cC_{n+2}(0)\ .$$

Equations (12)–(14) can be solved subject to the initial condition (15), and the resulting expressions, for the probability amplitudes are

$$C_{a,n}(t)=\left[\frac{g_1^2(n+1)}{\Lambda_n\alpha_n^2}\gamma_n+1\right]C_{a,n}(0) +\left[\frac{g_1g_2\sqrt{(n+1)(n+2)}}{\Lambda_n\alpha_n^2}\gamma_n\right]C_{c,n+2}(0)\ , \quad (16)$$

$$C_{b,n+1}(t)=-ig_1\frac{\sqrt{n+1}}{\Lambda_n}\eta_nC_{a,n}(0) -ig_2\frac{\sqrt{n+2}}{\Lambda_n}\eta_nC_{c,n+2}(0)\ , \quad (17)$$

$$C_{c,n+2}(t)=\left[\frac{g_1g_2\sqrt{(n+1)(n+2)}}{\Lambda_n\alpha_n^2}\gamma_n\right]C_{a,n}(0) +\left[\frac{g_2^2(n+2)}{\Lambda_n\alpha_n^2}\gamma_n+1\right]C_{c,n+2}(0)\ , \quad (18)$$

where

$$\alpha_n=[g_1^2(n+1)+g_2^2(n+2)]^{1/2}\ , \quad (19)$$

$$\Lambda_n=\left[\frac{\Delta^2}{4}+\alpha_n^2\right]^{1/2}\ , \quad (20)$$

$$\gamma_n=\left[\Lambda_n\cos\Lambda_nt+i\frac{\Delta}{2}\sin\Lambda_nt-\Lambda_n\exp\left[i\frac{\Delta}{2}t\right]\right] \times\exp\left[-i\frac{\Delta}{2}t\right]\ , \quad (21)$$

$$\eta_n=\sin\Lambda_nt\exp\left[i\frac{\Delta}{2}t\right]\ . \quad (22)$$

Here Λ_n is the Rabi frequency. Equations (16)–(18) give the probability amplitudes in the FMHA.

C. Comparison of the EHA with the FMHA

Now we determine the conditions under which the probability amplitudes obtained from the FMHA effectively reduce to those obtained from the EHA.

We consider a special case by taking

$$g_1=g_2=g\ , \quad (23)$$

which is an inherent property of the effective Hamiltonian. In order to facilitate the comparison between the two approaches we introduce an effective two-photon coupling constant

$$\lambda=\frac{g^2}{\Delta}\ , \quad (24)$$

and

$$\epsilon_n=\frac{4\lambda}{\Delta}(2n+3)\ . \quad (25)$$

The Rabi frequency Λ_n [cf. Eq. (20)] is given in terms of ϵ by the relation

$$\Lambda_n=\frac{\Delta}{2}(1+\epsilon_n)^{1/2}\ . \quad (26)$$

In order to retain the leading terms under the large-detuning limit, $\epsilon_n \ll 1$, in the expansion

$$\Lambda_n=\frac{\Delta}{2}\left[1+\frac{\epsilon_n}{2}-\frac{\epsilon_n^2}{8}+\cdots\right]\ , \quad (27)$$

which appears as an argument of trigonometric functions in Eqs. (16)–(18), we need to satisfy the condition

$$\frac{\epsilon_n^2}{16}\frac{\Delta}{\lambda}\lambda t \ll \pi\ . \quad (28)$$

We assume that $C_n(0)$ is a sharply peaked function of n about $n=\bar{n}$. We also assume

$$\bar{n}\gg 1\ . \quad (29)$$

We can then replace $n+1$, $n+2$, and $(2n+3)/2$ by $\sqrt{(n+1)(n+2)}$ in Eqs. (16)–(18). The inequality (28) then reduces to

$$\frac{\Delta}{\lambda}\gg\frac{4\bar{n}^2}{\pi}\lambda t\ , \quad (30)$$

which depends on the interaction time. This condition imposes a condition on the detuning for a particular choice of the photon number $\bar{n}$ and the interaction time λt. For small values of λt, the large-detuning limit $\epsilon_n \ll 1$ dictates another condition, i.e., $\Delta/\lambda \gg 4(2\bar{n}+3)$. This condition, however, becomes redundant when $\lambda t>\pi/\bar{n}$. Equations (16)–(18) for the probability amplitudes, under conditions (29) and (30), become

$$C_{a,n}(t)=\exp[i\sqrt{(n+1)(n+2)}\lambda t] \times\{\cos[\sqrt{(n+1)(n+2)}\lambda t]C_{a,n}(0) +i\sin[\sqrt{(n+1)(n+2)}\lambda t]C_{c,n+2}(0)\}\ , \quad (31)$$

$$C_{b,n+1}(t)=O(\sqrt{\epsilon/2}) \ . \tag{32}$$

$$C_{c,n+2}(t)=\exp[i\sqrt{(n+1)(n+2)}\lambda t] \times\{\cos[\sqrt{(n+1)(n+2)}\lambda t]C_{c,n+2}(0) + i\sin[\sqrt{(n+1)(n+2)}\lambda t]C_{a,n}(0)\} \ . \tag{33}$$

We observe that the probability of finding the atom in the atomic state $|b\rangle$ becomes negligibly small. Hence our three-level atom effectively reduced to a two-level atom at two-photon resonance. A comparison of Eqs. (31) and (33) with Eqs. (7) and (8) shows that, apart from an additional overall phase factor $\exp[i\sqrt{(n+1)(n+2)}\lambda t]$ in the FMHA, the solution for the probability amplitudes in the FMHA reduces to those in the EHA under the conditions (29) and (30). This intensity-dependent phase factor arises due to dynamic Stark shifts of the atomic levels which have been neglected in the EHA. In order to study the consequences of the difference due to the additional phase factor on various quantities of interest, we construct the density matrix of the combined atom and field system.

$$\rho_{AF}(t)=\sum_{n,m,\alpha,\beta} C_{\alpha,n}(t)C^*_{\beta,m}(t)|\alpha,n\rangle\langle\beta,m| \ , \tag{34}$$

where $\alpha,\beta=a,b,c$ corresponds to the atomic states. We observe that the additional overall phase factor can only play a role in the off-diagonal elements for the reduced density matrix of the field, while diagonal elements remain the same in both approaches. This point has already been observed in the case of lasers by Boone and Swain [12] and in the case of micromasers by Ashraf, Gea-Banacloche, and Zubairy [13].

1. Population inversion

Population inversion involves diagonal elements of the reduced density matrix for the field. We get the same result for the EHA and FMHA under the conditions (29) and (30). In the case of an initial coherent field having a mean number of photons $\bar{n}=50$, inequality (30) yields $\Delta/\lambda>>10\,000$. We gradually achieve this condition for the FMHA in Figs. 2(a)–2(c). In these figures we have plotted the population inversion $W(t)$ versus dimensionless time λt. The population inversion obtained from the EHA for $\bar{n}=50$, has been shown in Fig. 2(d). It is clear from Figs. 2(c) and 2(d) that, for small values of λt, both approaches exhibit identical behavior. For large values of interaction time, we get a somewhat different result. This happens because the inequality (30) breaks down for $\lambda t\sim(\Delta/\lambda)(\pi/4\bar{n}^2)$.

In case of an initial thermal field, which obeys the Boltzmann distribution, the maximum contribution comes from the small values of n. However, condition (29) can be fulfilled for large values of n. It is worthwhile to mention that most of the experimental work in the single-atom QED for the initial thermal field is done for very small values of $\bar{n}$ [6,14]. Hence one cannot use the EHA to deal with such a situation because of the violation of condition (29). In Fig. 3 we have plotted popula-

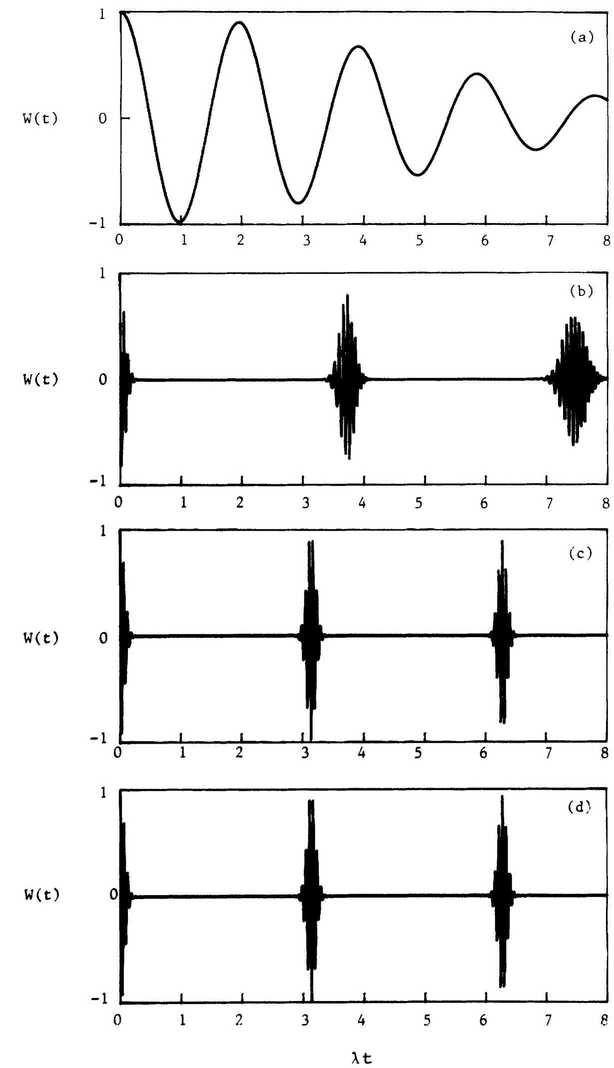

FIG. 2. $W(t)$ vs λt, for $\theta=0$, initial coherent field with $\bar{n}=50$, for (a) $\Delta/\lambda=0.1$, (b) $\Delta/\lambda=1000$, (c) $\Delta/\lambda=5\times10^5$ in the FMHA, and (d) corresponding curve in the EHA.

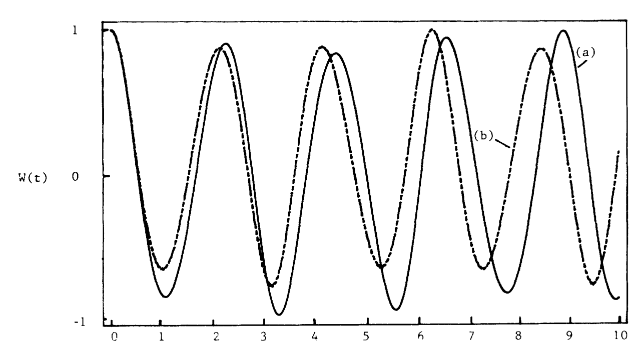

FIG. 3. $W(t)$ vs λt, for $\theta=0$, for initial thermal field with $\bar{n}=0.1$ (a) in the EHA, and (b) in the FMHA, for $\Delta/\lambda=500$.

tion inversion versus dimensionless time to see the difference between the EHA and the FMHA for $\bar{n}=0.1$.

2. Photon distribution function

The photon distribution function gives the probability of finding n photons at any time t. In the photon distribution function only the diagonal elements for the reduced density matrix of the field are involved. Hence the additional overall phase factor cancels out. It is evident that only the trace over atomic variables is carried out in Eq. (37). The conditions (29) and (30) are therefore modified by replacing $\bar{n}$ by n. This modification does not play any role in the case of initial coherent field for larger values of $\bar{n}$. As in the case of such distributions, the contribution given by small values of n is negligibly small. Hence we get identical results from both approaches under condition (30). However, for smaller values of $\bar{n}$, the small values of n attain considerable weightage in initial photon distribution. The two approaches therefore yield significantly different results for small values of n.

In the case of an initial thermal field, different results are obtained from the two approaches for small values of n, and even for large values of $\bar{n}$. This can be observed in Figs. 4(a) and 4(b), where $P(n)$ is plotted versus n for $\bar{n}=10$, for the EHA and FMHA, respectively. This can be explained by considering the fact that the thermal distribution peaks at $n=0$. The maximum contribution therefore comes from small values of n, where the modified condition (29) is violated. Identical results will be obtained from the two approaches for large values of n, under condition (30).

3. Squeezing

One of the major reasons for the recent interest in multiphoton processes is due to the high degree of correlation between the pairs of photons that result in squeezing. We introduce two Hermitian conjugate operators $a_1=(a+a^\dagger)/2$ and $a_2=(a-a^\dagger)/2i$ obeying the uncertainly relation

$$\Delta a_1 \Delta a_2 > \tfrac{1}{4} , \tag{35}$$

where

$$(\Delta a_1)^2=\tfrac{1}{4}(2\langle a^\dagger a\rangle+1+\langle a^2\rangle+\langle a^{\dagger 2}\rangle) - \tfrac{1}{4}\langle a+a^\dagger\rangle^2 , \tag{36}$$

$$(\Delta a_2)^2=\tfrac{1}{4}(2\langle a^\dagger a\rangle+1-\langle a^2\rangle-\langle a^{\dagger 2}\rangle) + \tfrac{1}{4}\langle a-a^\dagger\rangle^2 . \tag{37}$$

A state of the field is said to be squeezed when one of the quadratures a_1 or a_2 satisfies

$$(\Delta a_i)^2 < \tfrac{1}{4} , \quad i=1,2 . \tag{38}$$

The quantities $\langle a^2\rangle$, $\langle a^{\dagger 2}\rangle$, $\langle a+a^\dagger\rangle$, and $\langle a-a^\dagger\rangle$ in Eqs. (39) and (40) contain off-diagonal elements of the re-

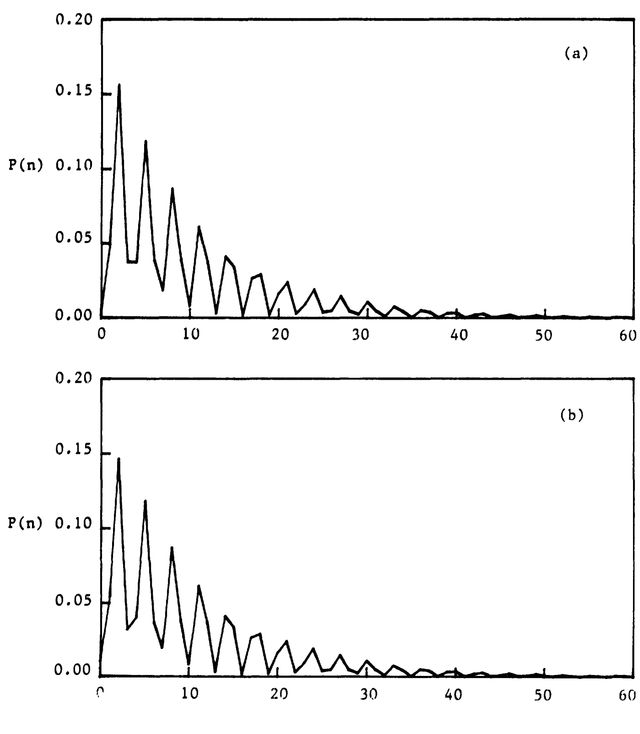

FIG. 4. $P(n)$ vs n, at $\lambda t=1$ for $\theta=0$, for initial thermal field with $\bar{n}=10$ (a) in the EHA, and (b) in the FMHA, for $\Delta/\lambda=1\times10^5$.

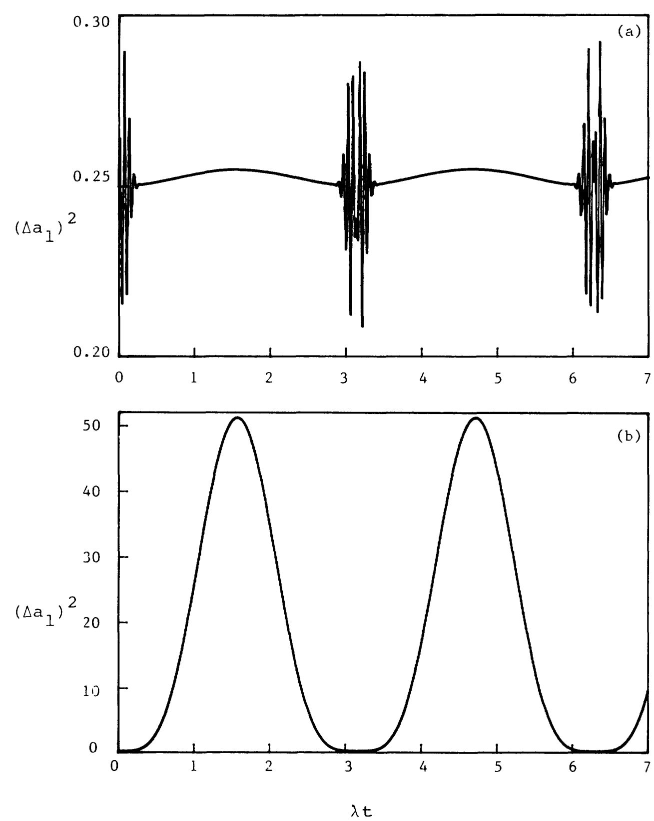

FIG. 5. $(\Delta a_1)^2$ vs λt, for $\theta=0$, for initial coherent field with $\bar{n}=50$, in high resolution about $\lambda t=\pi$ (a) in the EHA, and (b) in the FMHA, for $\Delta/\lambda=5\times10^5$.

duced density matrix of the field. In the case of the initial coherent field, $\bar{n}$ is taken to be large in order to satisfy condition (29). The behavior of $(\Delta a_1)^2$ vs λt in the EHA is presented in Fig. 5(a). The corresponding curve in the FMHA, in accordance with condition (30), i.e., $\Delta/\lambda = 50\,000$, is shown in Fig. 5(b). The square of the variance in the other quadrature, i.e., $(\Delta a_2)^2$, in both approaches is plotted versus λt in Fig. 7. It is clear from Fig. 5(a), 5(b), and (7) that both approaches, in general, exhibit drastically different results, which we may expect because of the additional overall phase factor in the FMHA.

These results, however, can be explained by considering the fact that the additional overall phase factor $\exp[i\sqrt{(n+1)(n+2)}\lambda t]$ approaches 1 for $n \gg 1$, for all those values of λt that are an integral multiple of π. Hence the phase factor does not play a significant role in these particular values of λt, thus giving almost identical results in the two approaches. When we move away from these values we start getting a contribution from the phase factor, see Figs. 6(a) and 6(b). The phase factor approaches -1 at those values of λt that are an odd integral multiple of $\pi/2$, to give a maximum difference in the behavior of two approaches. This argument is also supported by the results for $(\Delta a_2)^2$, where almost the reverse behavior is exhibited for the two approaches for these values of λt, see Fig. 7. We conclude from the above discussion that effective Hamiltonian is valid under certain conditions for the quantities in which diagonal elements of the field density matrix are involved. But for the quantities in which off-diagonal elements of the field density matrix are involved, the effective Hamiltonian need some modifications.

III. MODIFIED EFFECTIVE HAMILTONIAN APPROACH

The neglecting of the dynamic Stark shift in the effective Hamiltonian leads to a different result for the quantities in which the off-diagonal elements of the reduced density matrix are involved, such as squeezing. Consequently, a modified effective Hamiltonian is proposed [15] in which the dynamic Stark shift is taken care of by the inclusion of Stark parameters, i.e.,

$$H = \hbar\lambda(a^2|a\rangle\langle c| + a^{\dagger 2}|c\rangle\langle a|) - \hbar a^\dagger a(\beta_1|a\rangle\langle a| + \beta_2|c\rangle\langle c|) , \quad (39)$$

where β_1 and β_2 are dynamic Stark-shift parameters for atomic levels $|a\rangle$ and $|c\rangle$, respectively. Corresponding to this Hamiltonian, the solution of the probability amplitude equations subject to condition (5) is

$$C_{a,n}(t) = \exp(iV_n t)\{C_{a,n}(0)\cos(\Omega_n t) + (i/\Omega_n)[(n\beta_1 - V_n)C_{a,n}(0) - \lambda\sqrt{(n+1)(n+2)}C_{c,n+2}(0)]\sin(\Omega_n t)\} , \quad (40)$$

$$C_{c,n+2}(t) = \exp(iV_n t)\{C_{c,n+2}(0)\cos(\Omega_n t) - (i/\Omega_n)[(n\beta_1 - V_n)C_{c,n+2}(0) + \lambda\sqrt{(n+1)(n+2)}C_{a,n}(0)]\sin(\Omega_n t)\} , \quad (41)$$

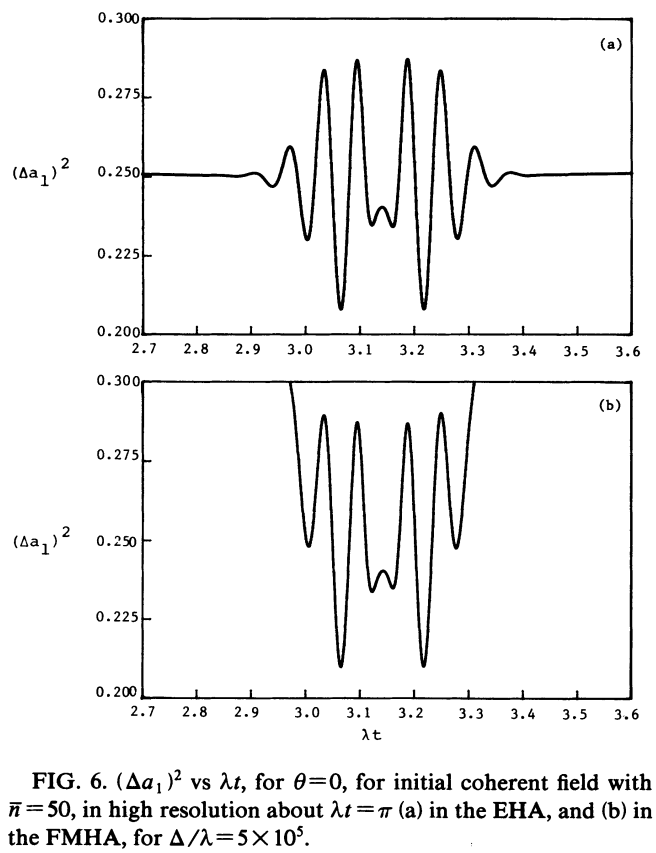

FIG. 6. $(\Delta a_1)^2$ vs λt, for $\theta = 0$, for initial coherent field with $\bar{n} = 50$, in high resolution about $\lambda t = \pi$ (a) in the EHA, and (b) in the FMHA, for $\Delta/\lambda = 5\times 10^5$.

where

$$V_n = \tfrac{1}{2}[n\beta_1 + (n+2)\beta_2] , \quad (42)$$

and

$$\Omega_n = \tfrac{1}{2}[(n\beta_1 - (n+2)\beta_2)^2 + 4\lambda(n+1)(n+2)]^{1/2} . \quad (43)$$

Now we compare the probability amplitude equations obtained from the MEHA with those corresponding to the FMHA, i.e., Eqs. (16)–(18). The validity of the modified effective Hamiltonian is determined by the con-

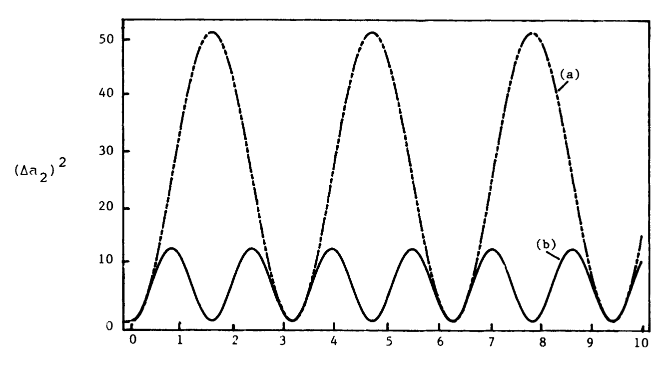

FIG. 7. $(\Delta a_2)^2$ vs λt, for $\theta = 0$, for initial coherent field with $\bar{n} = 50$ (a) in the EHA, and (b) in the FMHA, for $\Delta/\lambda = 5\times 10^5$.

ditions under which the MEHA and the FMHA give identical results for the probability amplitude equations. In the full microscopic Hamiltonian approach the Stark parameters β_1 and β_2 correspond to g_1^2/Δ and g_2^2/Δ, while the two-photon coupling constant λ is $g_1 g_2/\Delta$. Equations (19)–(22) can be written as

$$\alpha_n=[(n+1)\beta_1+(n+2)\beta_2]^{1/2}\Delta^{1/2}\ , \tag{44}$$

$$\Lambda_n=(1+\delta_n)^{1/2}\frac{\Delta}{2}\ , \tag{45}$$

$$\gamma_n=\frac{\Delta}{2}\left\{\cos\left[\frac{\Delta}{2}\left[1+\frac{\delta_n}{2}\right]t\right]+i\sin\left[\frac{\Delta}{2}\left[1+\frac{\delta_n}{2}\right]t\right]-\exp\left[i\frac{\Delta}{2}t\right]\right\}\exp\left[-i\frac{\Delta}{2}t\right]\ , \tag{46}$$

$$\eta_n=\sin\left[\frac{\Delta}{2}\left[1+\frac{\delta_n}{2}\right]t\right]\exp\left[i\frac{\Delta}{2}t\right]\ , \tag{47}$$

where

$$\delta_n=(4/\Delta)[(n+1)\beta_1+(n+2)\beta_2]\ . \tag{48}$$

Under the large-detuning limit, i.e., $\delta_n \ll 1$, the Rabi frequency Λ_n can be expanded. In order to retain just the leading terms in the trigonometric functions, we must have

$$\frac{1}{\Delta}\{[(n+1)\beta_1+(n+2)\beta_2]^2\}t \ll \pi\ . \tag{49}$$

The probability amplitude equations from the FMHA can be written as follows:

$$C_{a,n}(t)=\left[\frac{(n+1)\beta_1}{(n+1)\beta_1+(n+2)\beta_2}(\exp\{i[(n+1)\beta_1+(n+2)\beta_2]t\}-1)+1\right]C_{a,n}(0)$$
$$+\left[\frac{\lambda\sqrt{(n+1)(n+2)}}{(n+1)\beta_1+(n+2)\beta_2}(\exp\{i[(n+1)\beta_1+(n+2)\beta_2]t\}-1)\right]C_{c,n+2}(0)\ , \tag{50}$$

$$C_{b,n+1}(t)=-2\left[\frac{(n+1)\beta_1}{\Delta}\right]^{1/2}\eta_n C_{a,n}(0)-2\left[\frac{(n+2)\beta_2}{\Delta}\right]^{1/2}\eta_n C_{c,n+2}(0)\ , \tag{51}$$

$$C_{c,n+2}(t)=\left[\frac{\lambda\sqrt{(n+1)(n+2)}}{(n+1)\beta_1+(n+2)\beta_2}(\exp\{i[(n+1)\beta_1+(n+2)\beta_2]t\}-1)\right]C_{a,n}(0)$$
$$+\left[\frac{(n+2)\beta_2}{(n+1)\beta_1+(n+2)\beta_2}(\exp\{i[(n+1)\beta_1+(n+2)\beta_2]t\}-1)+1\right]C_{c,n+2}(0)\ . \tag{52}$$

Since β_1 and β_2 are of the same sign, then the large-detuning limit ($\delta_n \ll 1$) confirms that

$$\left[\frac{(n+1)\beta_1}{\Delta}\right]^{1/2},\ \left[\frac{(n+2)\beta_2}{\Delta}\right]^{1/2} \ll 1\ ,$$

which means that $C_{b,n+1}\approx 0$ (i.e., effective two-level atom). In the large-detuning limit, the one-photon Rabi frequency for the dipole-allowed transitions is completely suppressed by introducing detuning to the intermediate level $|b\rangle$ with respect to cavity resonant mode Ω. For $\bar{n}\gg 1$, Eqs. (42) and (43) gives $\Omega_n=V_n$, which leads to identical results from the MEHA and FMHA for the probability amplitude equations. The condition (49), in the limit $\bar{n}\gg 1$, can also be written in terms of dimensionless quantities as follows:

$$\frac{\bar{n}}{\pi}\left[\frac{(r^2+1)}{r}\right]^2\lambda t \ll \frac{\Delta}{\lambda}\ , \tag{53}$$

where

$$r=\frac{g_1}{g_2}\ . \tag{54}$$

Condition (53) reduced to (30) for $r=1$. However, if $r\neq 1$ then we have an additional factor $[(r^2+1)/r]^2$ on the left-hand side with respect to inequality (30). It can be seen from Eq. (54) that, for $r=0$ or ∞, the three-level atom reduces to a two-level atom coupled via the one-photon process.

The MEHA can be used to study the quantities in which both diagonal and off-diagonal elements of the density matrix are involved. We would get identical results for population inversion, and the photon distribution function, as well as for squeezing from the two approaches under the above-mentioned conditions. It is important to note that, in the case of an initial thermal field, the MEHA could only be used for large values of mean number of photons $\bar{n}$. But for small values of $\bar{n}$, which are of experimental interest [6,14] we cannot employ the MEHA. In the case of an initial thermal field, $(\Delta a_1)^2$ is plotted for $\bar{n}=0.1$ for both the MEHA and FMHA, see Fig. 8.

IV. SUMMARY

We have examined the validity of the effective Hamiltonian approach in the two-photon Jaynes-Cummings model by comparing it with the results obtained from the full microscopic Hamiltonian. The conditions have been

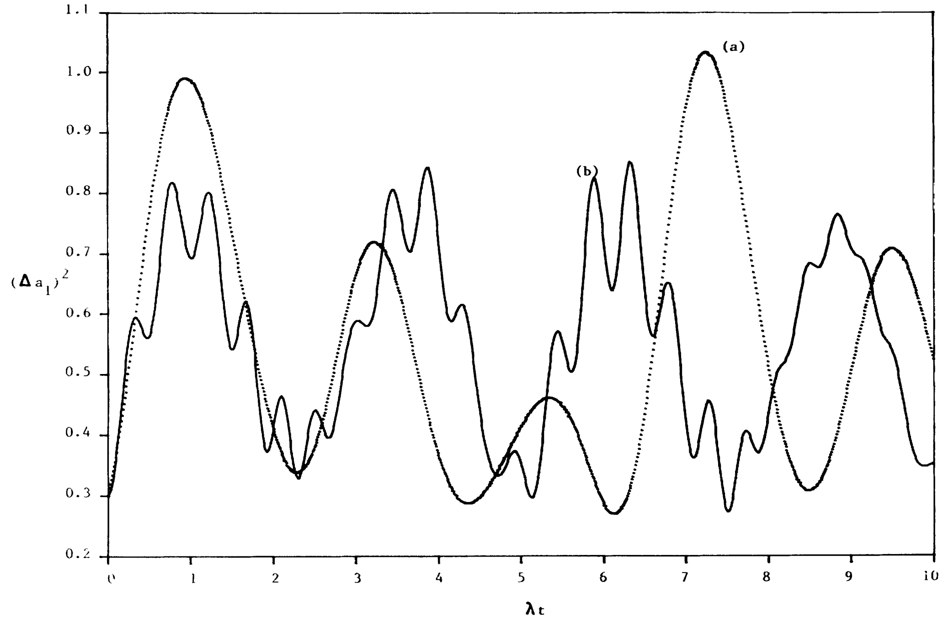

FIG. 8. $(\Delta a_1)^2$ vs λt for $\theta=\pi/2$, $\phi=\pi/2$ in the case of initial thermal field with $\bar{n}=0.1$ and $r=2.0$ (a) in the MEHA, and (b) in the FMHA, for $\Delta/\lambda=10$.

determined under which both Hamiltonian approaches yield identical results for the probability amplitudes apart from an additional overall phase factor. It has been shown that the quantities in which only the diagonal elements of the reduced density matrix for the field are involved, e.g., population inversion and the photon distribution function, identical results are obtained in the two approaches under these conditions. The two approaches, however, exhibit drastically different behavior for the variances of the quadrature components in which off-diagonal elements of the reduced density matrix for the field are involved, thus leading to substantially different results for squeezing. The additional phase factor in the FMHA arises from neglecting the dynamic Stark shift in the EHA. We then consider a modified effective Hamiltonian in which the dynamic Stark shift is taken care of. Our results clearly elucidate the conditions under which the modified effective Hamiltonian approach may be employed in the study of various quantities of interest in the two-photon atom-field interaction.

We have recently become aware of a paper by Barizis and Nayyak [17], in which comparison was made between the results predicted by the FMHA and the MEHA. Their results are, however, limited to relatively small detunings, where the predictions of the two Hamiltonians are different.

ACKNOWLEDGMENTS

This work is supported, in part, by grants from the Pakistan Science Foundation and the Pakistan Atomic Energy Commission.

[1] M. S. Zubairy, M. S. K. Razmi, S. Iqbal, and M. Idress, Phys. Lett. **98A**, 168 (1983).
[2] R. Loudon, Opt. Commun. **49**, 67 (1984).
[3] M. S. Zubairy, Phys. Lett. **87A**, 162 (1982).
[4] See, for example, R. Loudon *Quantum Theory of Light* (Clarendon, Oxford, 1983).
[5] H. D. Simann and R. Loudon, J. Phys. A **8**, 539 (1975); H. Paul, U. Mohr, and W. Brunner, Opt. Commun. **17**, 145 (1976); M. S. Zubairy and J. J. Yeh, Phys. Rev. A **21**, 1624 (1980); H. Voigt, A. Bandilla, and H. H. Ritze, Z. Phys. B **36**, 295 (1980).
[6] M. Brune, J. M. Raimond, P. Goy, L. Davidovich, and S. Haroche, Phys. Rev. Lett. **59**, 1899 (1987).
[7] S.-Y. Zhu and X.-S. Li, Phys. Rev. A **36**, 3889 (1987); S.-Y. Zhu and M.O. Scully, *ibid.* **38**, 5433 (1988).
[8] P. Alsing and M. S. Zubairy, J. Opt. Soc. Am. B **4**, 177 (1987).
[9] M. O. Scully, Phys. Rev. Lett. **55**, 2802 (1985); M. O. Scully and M. S. Zubairy, Phys. Rev. A **35**, 752 (1987); K. Zaheer and M. S. Zubairy, *ibid.* **38**, 5227 (1988); J. Bergou, M. Orszag, and M. O. Scully, Phys. Rev. A **38**, 754 (1988); M. O. Scully, K. Wodkiewicz, M. S. Zubairy, J. Bergou, N. Lu, and J. Meyer ter Vehn, Phys. Rev. Lett. **60**, 1832 (1988).
[10] M. O. Scully and M. S. Zubairy, Opt. Commun. **66**, 303 (1988); N. A. Ansari, J. Gea-Banacloche, and M. S. Zubairy, Phys. Rev. A **41**, 5179 (1990).
[11] L. Davidovich, J. M. Raimond, M. Brune, and S. Haroche, Phys. Rev. A **36**, 3771 (1987); I. Ashraf and M. S. Zubairy, Opt. Commun. **77**, 85 (1990).

[12] A. W. Boone and S. Swain, Opt. Commun. **73**, **47** (1989); A. W. Boone and S. Swain, Quantum Opt. **1**, 27 (1989).
[13] I. Ashraf, J. Gea-Banacloche, and M. S. Zubairy, Phys. Rev. A **42**, 6704 (1990).
[14] G. Rempe, H. Walther, and N. Klein, Phys. Rev. Lett. **58**, 353 (1987); D. Meschede, H. Walther, and G. Muller, *ibid.* **54**, 551 (1985).
[15] R. R. Puri and R. K. Bullough, J. Opt. Soc. Am. B **5**, 2021 (1988).
[16] L. A. Lugiato, P. Galatola, and L. M. Narducci, Opt. Commun. **76**, 276 (1990).
[17] V. Barizis and N. Nayak, J. Opt. Soc. Am. B **8**, 1779 (1991).